

PDF hosted at the Radboud Repository of the Radboud University Nijmegen

The following full text is a publisher's version.

For additional information about this publication click this link.

<http://repository.ubn.ru.nl/handle/2066/128265>

Please be advised that this information was generated on 2020-09-25 and may be subject to change.

Search for the decay of a B^0 or \bar{B}^0 meson to $\bar{K}^{*0}K^0$ or $K^{*0}\bar{K}^0$

B. Aubert, R. Barate, M. Bona, D. Boutigny, F. Couderc, Y. Karyotakis, J. P. Lees, V. Poireau, V. Tisserand, and A. Zghiche
Laboratoire de Physique des Particules, F-74941 Annecy-le-Vieux, France

E. Grauges

Universitat de Barcelona, Facultat de Fisica Dept. ECM, E-08028 Barcelona, Spain

A. Palano

Università di Bari, Dipartimento di Fisica and INFN, I-70126 Bari, Italy

J. C. Chen, N. D. Qi, G. Rong, P. Wang, and Y. S. Zhu

Institute of High Energy Physics, Beijing 100039, China

G. Eigen, I. Ofte, and B. Stugu

University of Bergen, Institute of Physics, N-5007 Bergen, Norway

G. S. Abrams, M. Battaglia, D. N. Brown, J. Button-Shafer, R. N. Cahn, E. Charles, M. S. Gill, Y. Groysman,
R. G. Jacobsen, J. A. Kadyk, L. T. Kerth, Yu. G. Kolomensky, G. Kukartsev, G. Lynch, L. M. Mir, P. J. Oddone,
T. J. Orimoto, M. Pripstein, N. A. Roe, M. T. Ronan, and W. A. Wenzel

Lawrence Berkeley National Laboratory and University of California, Berkeley, California 94720, USA

P. del Amo Sanchez, M. Barrett, K. E. Ford, T. J. Harrison, A. J. Hart, C. M. Hawkes, S. E. Morgan, and A. T. Watson

University of Birmingham, Birmingham, B15 2TT, United Kingdom

K. Goetzen, T. Held, H. Koch, B. Lewandowski, M. Pelizaeus, K. Peters, T. Schroeder, and M. Steinke

Ruhr Universität Bochum, Institut für Experimentalphysik 1, D-44780 Bochum, Germany

J. T. Boyd, J. P. Burke, W. N. Cottingham, and D. Walker

University of Bristol, Bristol BS8 1TL, United Kingdom

T. Cuhadar-Donszelmann, B. G. Fulsom, C. Hearty, N. S. Knecht, T. S. Mattison, and J. A. McKenna

University of British Columbia, Vancouver, British Columbia, Canada V6T 1Z1

A. Khan, P. Kyberd, M. Saleem, D. J. Sherwood, and L. Teodorescu

Brunel University, Uxbridge, Middlesex UB8 3PH, United Kingdom

V. E. Blinov, A. D. Bukin, V. P. Druzhinin, V. B. Golubev, A. P. Onuchin, S. I. Serednyakov, Yu. I. Skovpen,
E. P. Solodov, and K. Yu Todyshev

Budker Institute of Nuclear Physics, Novosibirsk 630090, Russia

D. S. Best, M. Bondioli, M. Bruinsma, M. Chao, S. Curry, I. Eschrich, D. Kirkby, A. J. Lankford, P. Lund, M. Mandelkern,
R. K. Mommsen, W. Roethel, and D. P. Stoker

University of California at Irvine, Irvine, California 92697, USA

S. Abachi and C. Buchanan

University of California at Los Angeles, Los Angeles, California 90024, USA

S. D. Foulkes, J. W. Gary, O. Long, B. C. Shen, K. Wang, and L. Zhang

University of California at Riverside, Riverside, California 92521, USA

H. K. Hadavand, E. J. Hill, H. P. Paar, S. Rahatlou, and V. Sharma

University of California at San Diego, La Jolla, California 92093, USA

J. W. Berryhill, C. Campagnari, A. Cunha, B. Dahmes, T. M. Hong, D. Kovalskyi, and J. D. Richman

University of California at Santa Barbara, Santa Barbara, California 93106, USA

T. W. Beck, A. M. Eisner, C. J. Flacco, C. A. Heusch, J. Kroseberg, W. S. Lockman, G. Nesom, T. Schalk, B. A. Schumm, A. Seiden, P. Spradlin, D. C. Williams, and M. G. Wilson

University of California at Santa Cruz, Institute for Particle Physics, Santa Cruz, California 95064, USA

J. Albert, E. Chen, A. Dvoretzkii, D. G. Hitlin, I. Narsky, T. Piatenko, F. C. Porter, A. Ryd, and A. Samuel
California Institute of Technology, Pasadena, California 91125, USA

R. Andreassen, G. Mancinelli, B. T. Meadows, and M. D. Sokoloff
University of Cincinnati, Cincinnati, Ohio 45221, USA

F. Blanc, P. C. Bloom, S. Chen, W. T. Ford, J. F. Hirschauer, A. Kreisel, U. Nauenberg, A. Olivas, W. O. Ruddick, J. G. Smith, K. A. Ulmer, S. R. Wagner, and J. Zhang
University of Colorado, Boulder, Colorado 80309, USA

A. Chen, E. A. Eckhart, A. Soffer, W. H. Toki, R. J. Wilson, F. Winklmeier, and Q. Zeng
Colorado State University, Fort Collins, Colorado 80523, USA

D. D. Altenburg, E. Feltresi, A. Hauke, H. Jasper, A. Petzold, and B. Spaan
Universität Dortmund, Institut für Physik, D-44221 Dortmund, Germany

T. Brandt, V. Klose, H. M. Lacker, W. F. Mader, R. Nogowski, J. Schubert, K. R. Schubert, R. Schwierz, J. E. Sundermann, and A. Volk
Technische Universität Dresden, Institut für Kern- und Teilchenphysik, D-01062 Dresden, Germany

D. Bernard, G. R. Bonneaud, P. Grenier,^{*} E. Latour, Ch. Thiebaux, and M. Verderi
Ecole Polytechnique, LLR, F-91128 Palaiseau, France

D. J. Bard, P. J. Clark, W. Gradl, F. Muheim, S. Playfer, A. I. Robertson, and Y. Xie
University of Edinburgh, Edinburgh EH9 3JZ, United Kingdom

M. Andreotti, D. Bettoni, C. Bozzi, R. Calabrese, G. Cibinetto, E. Luppi, M. Negrini, A. Petrella, L. Piemontese, and E. Prencipe
Università di Ferrara, Dipartimento di Fisica and INFN, I-44100 Ferrara, Italy

F. Anulli, R. Baldini-Ferroli, A. Calcaterra, R. de Sangro, G. Finocchiaro, S. Pacetti, P. Patteri, I. M. Peruzzi,[†] M. Piccolo, M. Rama, and A. Zallo
Laboratori Nazionali di Frascati dell'INFN, I-00044 Frascati, Italy

A. Buzzo, R. Capra, R. Contri, M. Lo Vetere, M. M. Macri, M. R. Monge, S. Passaggio, C. Patrignani, E. Robutti, A. Santroni, and S. Tosi
Università di Genova, Dipartimento di Fisica and INFN, I-16146 Genova, Italy

G. Brandenburg, K. S. Chaisanguanthum, M. Morii, and J. Wu
Harvard University, Cambridge, Massachusetts 02138, USA

R. S. Dubitzky, J. Marks, S. Schenk, and U. Uwer
Universität Heidelberg, Physikalisches Institut, Philosophenweg 12, D-69120 Heidelberg, Germany

W. Bhimji, D. A. Bowerman, P. D. Dauncey, U. Egede, R. L. Flack, J. A. Nash, M. B. Nikolich, and W. Panduro Vazquez
Imperial College London, London, SW7 2AZ, United Kingdom

X. Chai, M. J. Charles, U. Mallik, N. T. Meyer, and V. Ziegler
University of Iowa, Iowa City, Iowa 52242, USA

J. Cochran, H. B. Crawley, L. Dong, V. Eyges, W. T. Meyer, S. Prell, E. I. Rosenberg, and A. E. Rubin
Iowa State University, Ames, Iowa 50011-3160, USA

A. V. Gritsan

Johns Hopkins University, Baltimore, Maryland 21218, USA

M. Fritsch and G. Schott

Universität Karlsruhe, Institut für Experimentelle Kernphysik, D-76021 Karlsruhe, Germany

N. Arnaud, M. Davier, G. Grosdidier, A. Höcker, F. Le Diberder, V. Lepeltier, A. M. Lutz, A. Oyanguren, S. Pruvot, S. Rodier, P. Roudeau, M. H. Schune, A. Stocchi, W. F. Wang, and G. Wormser

Laboratoire de l'Accélérateur Linéaire, IN2P3-CNRS et Université Paris-Sud 11, Centre Scientifique d'Orsay, B.P. 34, F-91898 ORSAY Cedex, France

C. H. Cheng, D. J. Lange, and D. M. Wright

Lawrence Livermore National Laboratory, Livermore, California 94550, USA

C. A. Chavez, I. J. Forster, J. R. Fry, E. Gabathuler, R. Gamet, K. A. George, D. E. Hutchcroft, D. J. Payne, K. C. Schofield, and C. Touramanis

University of Liverpool, Liverpool L69 7ZE, United Kingdom

A. J. Bevan, F. Di Lodovico, W. Menges, and R. Sacco

Queen Mary, University of London, E1 4NS, United Kingdom

G. Cowan, H. U. Flaecher, D. A. Hopkins, P. S. Jackson, T. R. McMahon, S. Ricciardi, F. Salvatore, and A. C. Wren

University of London, Royal Holloway and Bedford New College, Egham, Surrey TW20 0EX, United Kingdom

D. N. Brown and C. L. Davis

University of Louisville, Louisville, Kentucky 40292, USA

J. Allison, N. R. Barlow, R. J. Barlow, Y. M. Chia, C. L. Edgar, G. D. Lafferty, M. T. Naisbit, J. C. Williams, and J. I. Yi

University of Manchester, Manchester M13 9PL, United Kingdom

C. Chen, W. D. Hulsbergen, A. Jawahery, C. K. Lae, D. A. Roberts, and G. Simi

University of Maryland, College Park, Maryland 20742, USA

G. Blaylock, C. Dallapiccola, S. S. Hertzbach, X. Li, T. B. Moore, S. Saremi, H. Staengle, and S. Y. Willocq

University of Massachusetts, Amherst, Massachusetts 01003, USA

R. Cowan, G. Sciolla, S. J. Sekula, M. Spitznagel, F. Taylor, and R. K. Yamamoto

Massachusetts Institute of Technology, , USALaboratory for Nuclear Science, Cambridge, Massachusetts 02139, USA

H. Kim, P. M. Patel, and S. H. Robertson

McGill University, Montréal, Québec, Canada H3A 2T8

A. Lazzaro, V. Lombardo, and F. Palombo

Università di Milano, Dipartimento di Fisica and INFN, I-20133 Milano, Italy

J. M. Bauer, L. Cremaldi, V. Eschenburg, R. Godang, R. Kroeger, D. A. Sanders, D. J. Summers, and H. W. Zhao

University of Mississippi, University, Mississippi 38677, USA

S. Brunet, D. Côté, P. Taras, and F. B. Viaud

Université de Montréal, Physique des Particules, Montréal, Québec, Canada H3C 3J7

H. Nicholson

Mount Holyoke College, South Hadley, Massachusetts 01075, USA

N. Cavallo,[‡] G. De Nardo, F. Fabozzi,[‡] C. Gatto, L. Lista, D. Monorchio, P. Paolucci, D. Piccolo, and C. Sciacca

Università di Napoli Federico II, Dipartimento di Scienze Fisiche and INFN, I-80126, Napoli, Italy

M. Baak, G. Raven, and H. L. Snoek

NIKHEF, National Institute for Nuclear Physics and High Energy Physics, NL-1009 DB Amsterdam, The Netherlands

C. P. Jessop and J. M. LoSecco

University of Notre Dame, Notre Dame, Indiana 46556, USA

T. Allmendinger, G. Benelli, K. K. Gan, K. Honscheid, D. Hufnagel, P. D. Jackson, H. Kagan, R. Kass, A. M. Rahimi, R. Ter-Antonyan, and Q. K. Wong

Ohio State University, Columbus, Ohio 43210, USA

N. L. Blount, J. Brau, R. Frey, O. Igonkina, M. Lu, C. T. Potter, R. Rahmat, N. B. Sinev, D. Strom, J. Strube, and E. Torrence

University of Oregon, Eugene, Oregon 97403, USA

F. Galeazzi, A. Gaz, M. Margoni, M. Morandin, A. Pompili, M. Posocco, M. Rotondo, F. Simonetto, R. Stroili, and C. Voci

Università di Padova, Dipartimento di Fisica and INFN, I-35131 Padova, Italy

M. Benayoun, J. Chauveau, P. David, L. Del Buono, Ch. de la Vaissière, O. Hamon, B. L. Hartfiel, M. J. J. John, J. Malcèlès, J. Ocariz, L. Roos, and G. Therin

Universités Paris VI et VII, Laboratoire de Physique Nucléaire et de Hautes Energies, F-75252 Paris, France

P. K. Behera, L. Gladney, and J. Panetta

University of Pennsylvania, Philadelphia, Pennsylvania 19104, USA

M. Biasini, R. Covarelli, and M. Pioppi

Università di Perugia, Dipartimento di Fisica and INFN, I-06100 Perugia, Italy

C. Angelini, G. Batignani, S. Bettarini, F. Bucci, G. Calderini, M. Carpinelli, R. Cenci, F. Forti, M. A. Giorgi, A. Lusiani, G. Marchiori, M. A. Mazur, M. Morganti, N. Neri, G. Rizzo, and J. Walsh

Università di Pisa, Dipartimento di Fisica, Scuola Normale Superiore and INFN, I-56127 Pisa, Italy

M. Haire, D. Judd, and D. E. Wagoner

Prairie View A&M University, Prairie View, Texas 77446, USA

J. Biesiada, N. Danielson, P. Elmer, Y. P. Lau, C. Lu, J. Olsen, A. J. S. Smith, and A. V. Telnov

Princeton University, Princeton, New Jersey 08544, USA

F. Bellini, G. Cavoto, A. D'Orazio, D. del Re, E. Di Marco, R. Faccini, F. Ferrarotto, F. Ferroni, M. Gaspero, L. Li Gioi, M. A. Mazzoni, S. Morganti, G. Piredda, F. Polci, F. Safai Tehrani, and C. Voena

Università di Roma La Sapienza, Dipartimento di Fisica and INFN, I-00185 Roma, Italy

M. Ebert, H. Schröder, and R. Waldi

Universität Rostock, D-18051 Rostock, Germany

T. Adye, N. De Groot, B. Franek, E. O. Olaiya, and F. F. Wilson

Rutherford Appleton Laboratory, Chilton, Didcot, Oxon, OX11 0QX, United Kingdom

S. Emery, A. Gaidot, S. F. Ganzhur, G. Hamel de Monchenault, W. Kozanecki, M. Legendre, G. Vasseur, Ch. Yèche, and M. Zito

DSM/Daphnia, CEA/Saclay, F-91191 Gif-sur-Yvette, France

X. R. Chen, H. Liu, W. Park, M. V. Purohit, and J. R. Wilson

University of South Carolina, Columbia, South Carolina 29208, USA

M. T. Allen, D. Aston, R. Bartoldus, P. Bechtel, N. Berger, A. M. Boyarski, R. Claus, J. P. Coleman, M. R. Convery, M. Cristinziani, J. C. Dingfelder, J. Dorfan, G. P. Dubois-Felsmann, D. Dujmic, W. Dunwoodie, R. C. Field, T. Glanzman, S. J. Gowdy, M. T. Graham, V. Halyo, C. Hast, T. Hryn'ova, W. R. Innes, M. H. Kelsey, P. Kim, D. W. G. S. Leith, S. Li,

S. Luitz, V. Luth, H. L. Lynch, D. B. MacFarlane, H. Marsiske, R. Messner, D. R. Muller, C. P. O'Grady, V. E. Ozcan, A. Perazzo, M. Perl, T. Pulliam, B. N. Ratcliff, A. Roodman, A. A. Salnikov, R. H. Schindler, J. Schwiening, A. Snyder, J. Stelzer, D. Su, M. K. Sullivan, K. Suzuki, S. K. Swain, J. M. Thompson, J. Va'vra, N. van Bakel, M. Weaver, A. J. R. Weinstein, W. J. Wisniewski, M. Wittgen, D. H. Wright, A. K. Yarritu, K. Yi, and C. C. Young
Stanford Linear Accelerator Center, Stanford, California 94309, USA

P. R. Burchat, A. J. Edwards, S. A. Majewski, B. A. Petersen, C. Roat, and L. Wilden
Stanford University, Stanford, California 94305-4060, USA

S. Ahmed, M. S. Alam, R. Bula, J. A. Ernst, V. Jain, B. Pan, M. A. Saeed, F. R. Wappler, and S. B. Zain
State University of New York, Albany, New York 12222, USA

W. Bugg, M. Krishnamurthy, and S. M. Spanier
University of Tennessee, Knoxville, Tennessee 37996, USA

R. Eckmann, J. L. Ritchie, A. Satpathy, C. J. Schilling, and R. F. Schwitters
University of Texas at Austin, Austin, Texas 78712, USA

J. M. Izen, I. Kitayama, X. C. Lou, and S. Ye
University of Texas at Dallas, Richardson, Texas 75083, USA

F. Bianchi, F. Gallo, and D. Gamba
Università di Torino, Dipartimento di Fisica Sperimentale and INFN, I-10125 Torino, Italy

M. Bomben, L. Bosisio, C. Cartaro, F. Cossutti, G. Della Ricca, S. Dittongo, S. Grancagnolo, L. Lanceri, and L. Vitale
Università di Trieste, Dipartimento di Fisica and INFN, I-34127 Trieste, Italy

V. Azzolini and F. Martinez-Vidal
IFIC, Universitat de Valencia-CSIC, E-46071 Valencia, Spain

Sw. Banerjee, B. Bhuyan, C. M. Brown, D. Fortin, K. Hamano, R. Kowalewski, I. M. Nugent, J. M. Roney, and R. J. Sobie
University of Victoria, Victoria, British Columbia, Canada V8W 3P6

J. J. Back, P. F. Harrison, T. E. Latham, G. B. Mohanty, and M. Pappagallo
Department of Physics, University of Warwick, Coventry CV4 7AL, United Kingdom

H. R. Band, X. Chen, B. Cheng, S. Dasu, M. Datta, K. T. Flood, J. J. Hollar, P. E. Kutter, B. Mellado, A. Mihalyi, Y. Pan, M. Pierini, R. Prepost, S. L. Wu, and Z. Yu
University of Wisconsin, Madison, Wisconsin 53706, USA

H. Neal

Yale University, New Haven, Connecticut 06511, USA
 (Received 22 June 2006; published 23 October 2006)

We present a search for the decay of a B^0 or \bar{B}^0 meson to a $\bar{K}^{*0}K^0$ or $K^{*0}\bar{K}^0$ final state, using a sample of approximately 232×10^6 $B\bar{B}$ events collected with the *BABAR* detector at the PEP-II asymmetric energy e^+e^- collider at SLAC. The measured branching fraction is $\mathcal{B}(B^0 \rightarrow \bar{K}^{*0}K^0) + \mathcal{B}(B^0 \rightarrow K^{*0}\bar{K}^0) = (0.2_{-0.8-0.3}^{+0.9+0.1}) \times 10^{-6}$. We obtain the following upper limit for the branching fraction at 90% confidence level: $\mathcal{B}(B^0 \rightarrow \bar{K}^{*0}K^0) + \mathcal{B}(B^0 \rightarrow K^{*0}\bar{K}^0) < 1.9 \times 10^{-6}$. We use our result to constrain the standard model prediction for the deviation of the CP asymmetry in $B^0 \rightarrow \phi K^0$ from $\sin 2\beta$.

DOI: [10.1103/PhysRevD.74.072008](https://doi.org/10.1103/PhysRevD.74.072008)

PACS numbers: 13.25.Hw, 11.30.Er, 12.15.Hh

*Also at Laboratoire de Physique Corpusculaire, Clermont-Ferrand, France

†Also with Università di Perugia, Dipartimento di Fisica, Perugia, Italy

‡Also with Università della Basilicata, Potenza, Italy

I. INTRODUCTION

This paper describes a search for the decay of a B^0 or \bar{B}^0 meson to a $\bar{K}^{*0}K^0$ or $K^{*0}\bar{K}^0$ final state. Henceforth, we use $B^0 \rightarrow \bar{K}^{*0}K^0$ to refer to both B^0 and \bar{B}^0 decays and to the $\bar{K}^{*0}K^0$ and $K^{*0}\bar{K}^0$ decay channels. In the standard model (SM), $B^0 \rightarrow \bar{K}^{*0}K^0$ decays are described by the $b \rightarrow ds\bar{s}$ ‘‘penguin’’ diagrams shown in Fig. 1.

The SM prediction for the branching fraction of $B^0 \rightarrow \bar{K}^{*0}K^0$ is about 0.5×10^{-6} [1–3]. Extensions to the SM can yield significantly larger branching fractions, however. For example, models incorporating supersymmetry with R -parity violating interactions predict branching fractions as large as about 8×10^{-6} [3]. The event rates corresponding to this latter prediction are well within present experimental sensitivity. Currently, there are no experimental results for $B^0 \rightarrow \bar{K}^{*0}K^0$. Searches for the related nonresonant decay $B^0 \rightarrow K^- \pi^+ K^0$ are reported in Ref. [4].

At present, little experimental information is available for $b \rightarrow d$ transitions. Such processes can provide important tests of the quark-flavor sector of the SM as discussed, for example, in Ref. [5]. Our study is also relevant for the interpretation of the time dependent CP asymmetry obtained from $B^0 \rightarrow \phi K^0$ decays. To leading order, the CP asymmetry in $B^0 \rightarrow \phi K^0$ equals $\sin 2\beta$, but subdominant processes, proportional to the CKM matrix element V_{ub} , could produce a deviation $\Delta S_{\phi K^0}$, mimicking a signal for physics beyond the SM (for a review, see Sec. 12 of Ref. [6]). Exploiting $SU(3)$ flavor symmetry, Grossman *et al.* [7] introduced a method to combine the branching fractions of 11 B^0 decay channels to obtain a SM bound on $\Delta S_{\phi K^0}$. Of the 11 channels, experimental upper limits exist for all except $\bar{K}^{*0}K^0$ and $K^{*0}\bar{K}^0$, the topic of this study.

II. THE BABAR DETECTOR AND DATASET

The data used in this analysis were collected with the BABAR detector at the PEP-II asymmetric e^+e^- storage ring. The data sample consists of an integrated luminosity of 210 fb^{-1} recorded at the $Y(4S)$ resonance with a center-of-mass (CM) energy of $\sqrt{s} = 10.58 \text{ GeV}$, corresponding to $(232 \pm 2) \times 10^6 B\bar{B}$ events. A data sample of 21.6 fb^{-1} with a CM energy 40 MeV below the $Y(4S)$ resonance is used to study background contributions from continuum events, $e^+e^- \rightarrow q\bar{q}$ ($q = u, d, s$ or c).

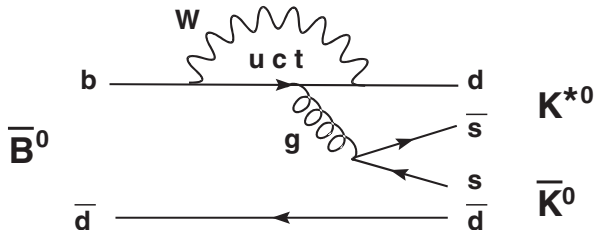


FIG. 1. Feynman diagrams for $\bar{B}^0 \rightarrow K^{*0}\bar{K}^0$.

The BABAR detector is described in detail elsewhere [8]. Charged particle tracks are reconstructed using a five-layer silicon vertex tracker (SVT) and a 40-layer drift chamber (DCH) immersed in a 1.5 T magnetic field. Tracks are identified as charged pions or kaons (particle identification) based on likelihoods constructed from specific energy loss measurements in the SVT and DCH and from Cherenkov radiation angles measured in the detector of internally reflected Cherenkov light. Photons are reconstructed from showers measured in the electromagnetic calorimeter. Muon and neutral hadron identification are performed with the instrumented flux return.

Monte Carlo (MC) events are used to determine signal and background characteristics, optimize selection criteria, and evaluate efficiencies. $B^0\bar{B}^0$ and B^+B^- events, and continuum events, are simulated with the EvtGen [9] and Jetset [10] event generators, respectively. The effective integrated luminosity of the MC samples is at least 4 times larger than that of the data for the $B^0\bar{B}^0$ and B^+B^- samples, and about 1.5 times that of the data for the continuum samples. Separate samples of specific $B^0\bar{B}^0$ decay channels are studied for the purposes of background evaluation. All MC samples include simulation of the BABAR detector response [11].

III. ANALYSIS METHOD

A. Event selection

$B^0 \rightarrow \bar{K}^{*0}K^0$ event candidates are identified through $K^{*0} \rightarrow K^+\pi^-$ and $K^0 \rightarrow K_S^0 \rightarrow \pi^+\pi^-$ decays. Throughout this paper, the charge conjugate channels are implied unless otherwise noted.

The initial event selection consists of the following. Events are required to contain at least five charged tracks and less than 20 GeV of total energy. These two selection criteria discriminate against backgrounds such as tau-pair, two-photon and cosmic ray events, and are essentially 100% efficient for well measured signal events. K_S^0 candidates are formed by combining all oppositely charged pairs of tracks, by fitting the two tracks to a common vertex, and by requiring the pair to have a fitted invariant mass within $0.025 \text{ GeV}/c^2$ of the nominal K_S^0 mass assuming the two particles to be pions. The K_S^0 candidate is combined in a vertex fit with two other oppositely charged tracks, associated with the K^{*0} decay, to form a B^0 candidate. These latter two tracks are each required to have a distance of closest approach to the e^+e^- collision point of less than 1.5 cm in the plane perpendicular to the beam axis and 10 cm along the beam axis. The χ^2 probability of the fitted B^0 vertex is required to exceed 0.003.

Our study utilizes an extended maximum likelihood (ML) technique to determine the number of signal and background events (Sec. III C). The fitted experimental variables are ΔE , m_{ES} , and the mass of the K^{*0} candidate $M_{K^+\pi^-}$, with $\Delta E \equiv E_B^* - E_{\text{beam}}^*$ and $m_{\text{ES}} \equiv \sqrt{E_{\text{beam}}^{*2} - P_B^{*2}}$

[8], where E_B^* and P_B^* are the CM energy and momentum of the B^0 candidate and E_{beam}^* is half the CM energy. $M_{K^+\pi^-}$ is determined by fitting the tracks from the K^{*0} candidate to a common vertex. We require events entering the ML fit to appear within a ‘‘fit window’’ defined by $|\Delta E| < 0.15$ GeV, $5.2 < m_{\text{ES}} < 5.3$ GeV/ c^2 , and $0.72 < M_{K^+\pi^-} < 1.20$ GeV/ c^2 . Virtually all well reconstructed signal events satisfy these criteria.

We further impose the following restrictions, optimized to minimize the estimated upper limit on the $B^0 \rightarrow \bar{K}^{*0} K^0$ branching fraction. The optimization is performed by comparing the expected number of signal [2] and background events as the selection values are changed.

The χ^2 probability of the fitted K_S^0 vertex is required to exceed 0.06. The fitted K_S^0 mass is required to lie within 10.5 MeV/ c^2 of the peak of the reconstructed K_S^0 mass distribution. (One standard deviation of the K_S^0 mass resolution is about 3 MeV/ c^2 .) The K_S^0 decay length significance, defined by the distance between the K^{*0} and K_S^0 decay vertices divided by the uncertainty on that quantity, is required to be larger than 3. The angle between the K_S^0 flight direction and its momentum vector, $\theta_{K_S^0}$, is required to satisfy $\cos\theta_{K_S^0} > 0.997$.

K^{*0} candidates are required to satisfy $|\cos\theta_H| > 0.50$, where θ_H is the helicity angle in the K^{*0} rest frame, defined as the angle between the direction of the boost from the B^0 rest frame and the K^+ momentum.

Of the two tracks associated with the K^{*0} decay, one is required to be identified as a kaon and the other as a pion using the particle identification. Charged kaons are identified with an efficiency and purity of about 80% and 90%, respectively, averaged over momentum. The corresponding values for charged pions are 90% and 80%. The efficiencies vary by less than 10% over the kinematic regions relevant for this analysis, and the purities by less than 5%.

B^0 mesons in $Y(4S)$ decays are produced almost at rest whereas continuum events at the $Y(4S)$ energy are characterized by jetlike structure. To suppress the dominant background arising from the continuum, we calculate the Legendre polynomial-like terms L_0 and L_2 defined by [12] $L_0 = \sum_{\text{r.o.e.}} p_i$ and $L_2 = \sum_{\text{r.o.e.}} \frac{p_i}{2} (3\cos^2\theta_i - 1)$, where p_i

is the magnitude of the 3-momentum of a particle and θ_i is its polar angle with respect to the thrust [13] axis, with the latter determined using the candidate B^0 decay products only. These sums are performed over all particles in the event not associated with the B^0 decay (‘‘rest-of-event’’ or r.o.e.). L_0 and L_2 are evaluated in the CM frame. We require $0.374L_0 - 1.179L_2 > 0.15$. The coefficients of L_0 and L_2 are determined with the Fisher discriminant method [14]. To further suppress the continuum background, we require $|\cos\theta_T| < 0.55$, where θ_T is the angle between the momentum of the B^0 candidate and the thrust axis, evaluated in the CM frame, with the thrust axis in this case determined from the r.o.e. particles.

After applying the above criteria, 3.8% of the selected events are found to contain more than one B^0 candidate. For these events, only the candidate with the largest B^0 vertex fit probability is retained.

The efficiencies obtained at the principal steps of the selection process are listed in Table I.

B. Background evaluation

To identify residual backgrounds from B decays that mimic characteristics of our signal, we examine $B^0\bar{B}^0$ MC events that satisfy the selection criteria of Sec. III A and that fall within the expected signal region of the m_{ES} distribution, defined by $5.271 < m_{\text{ES}} < 5.286$ GeV/ c^2 . We thereby identify the following three categories of background events.

- (1) Events containing B^0 decays with the same $K\pi\pi\pi$ final state as the signal. These channels are expected to peak in the signal regions of m_{ES} and ΔE but not in the signal region of $M_{K^+\pi^-}$. The largest number of background events in this category arises from $B^0 \rightarrow D^+ K^\pm (D^- \rightarrow \pi^- K_S^0)$. To reduce the contributions of this channel, we apply a veto on the $\pi^- K_S^0$ mass $M_{\pi K_S^0}$ based on the invariant mass of the K_S^0 and the pion used to reconstruct the K^{*0} . A veto with $1.813 < M_{\pi K_S^0} < 1.925$ GeV/ c^2 (corresponding to ± 7 standard deviations of a Gaussian fit to the $M_{\pi K_S^0}$ MC distribution) removes $64 \pm 1\%$ of the $D^\mp K^\pm$ background MC events where the

TABLE I. Event selection efficiencies for signal and background events, determined using Monte Carlo samples. The event numbers given for the background samples are adjusted to correspond to the integrated luminosity of the data. Event shape criteria refer to the requirements on L_0 , L_2 and $\cos\theta_T$ described in the text. The D^\mp and ϕ mass vetos are discussed in Sec. III B.

	Signal efficiency	$B^0\bar{B}^0$ events	B^+B^- events	$u\bar{u}, d\bar{d}, s\bar{s}, c\bar{c}$ events
Initial sample	100%	115×10^6	115×10^6	711×10^6
Initial selection and fit window	63%	12 100	14 700	2.12×10^6
K_S^0 criteria	54%	3290	1850	614 000
K^{*0} criteria	45%	2190	985	326 000
Particle identification	31%	159	114	57 200
Event Shape criteria	10%	39	27	700
D^\mp and ϕ mass vetos	9.8%	33	26	653

uncertainty is statistical. Note that the reconstructed $M_{\pi K_S^0}$ distribution has non-Gaussian tails.

- (2) Events containing B^0 decays with a kaon misidentified as a pion. This category of background is expected to peak in the m_{ES} signal region, but not in the $M_{K^+\pi^-}$ signal region, and to exhibit a peak in ΔE that is negatively displaced with respect to the signal peak centered at zero. The largest number of events in this category arises from $B^0 \rightarrow \phi K_S^0 (\phi \rightarrow K^+ K^-)$. We apply a veto on the $K^+ K^-$ mass $M_{K^+ K^-}$ assuming the pion candidate used to reconstruct the K^{*0} to be a kaon. The veto requires $1.0098 < M_{K^+ K^-} < 1.0280 \text{ GeV}/c^2$ (corresponding to ± 2.5 standard deviations of a Gaussian fit to the $M_{K^+ K^-}$ MC distribution). This selection requirement eliminates $87 \pm 1\%$ of the ϕK_S^0 background MC events.
- (3) Events containing B^0 decays with a pion misidentified as a kaon, such as $B^0 \rightarrow D^\pm \pi^\mp (D^\pm \rightarrow \pi^\pm K_S^0)$ or $B^0 \rightarrow \rho^0 K_S^0 (\rho^0 \rightarrow \pi^\pm \pi^\mp)$. This category of background peaks in the m_{ES} signal region but not in the $M_{K^+\pi^-}$ signal region and exhibits a peak in ΔE that is positively displaced from zero. A fourth category of $B\bar{B}$ background events is identified as follows.
- (4) All $B^0\bar{B}^0$ and B^+B^- MC events that satisfy the selection criteria of Sec. III A but that do not fall into the three categories listed above. These events are characterized both by particle misidentification and an exchange of tracks between the B and \bar{B} decays. This class of events does not peak in ΔE . Based on scaling to the experimental luminosity, 1 event (rounded to the nearest integer) is expected for each of the first three categories, and 54 events for the fourth category. We also consider potential background from the following source.
- (5) Events with the same $K\pi\pi\pi$ final state as our signal but with a $K^\pm\pi^\mp$ S -wave decay amplitude, either nonresonant or produced, e.g., through $B^0 \rightarrow K_0^{*0}(1430)K_S^0 (K_0^{*0}(1430) \rightarrow K^\pm\pi^\mp)$ decays. These channels are expected to peak in the signal regions of m_{ES} and ΔE but not in the signal region of $M_{K^+\pi^-}$.

There are no experimental results for $B^0 \rightarrow K_0^{*0}(1430)K_S^0$. Studies [15] of $B^+ \rightarrow K^+\pi^+\pi^-$ found a substantial $B^+ \rightarrow K_0^{*0}(1430)\pi^+$ resonant component, however. To evaluate this potential source of background, we generate $B^0 \rightarrow K_0^{*0}(1430)K_S^0 (K_0^{*0}(1430) \rightarrow K^+\pi^-)$ MC events. After applying the criteria described in Sec. III A, only $1.4 \pm 0.1\%$ of these events remain. More importantly, the interference between the $K^{*0}(890)$ and S -wave $K\pi$ amplitudes is expected to cancel if the detection efficiency is symmetric in the candidate $K^{*0} \cos\theta_H$ distribution. Through MC study, we verify that our efficiency is symmetric in $\cos\theta_H$ to better than about 10%. This allows us to treat potential

S -wave $K^\pm\pi^\mp$ background as an independent component in the ML fit.

C. Fit procedure

An unbinned extended maximum likelihood fit is used to determine the number of signal and background events in the data. The extended likelihood function \mathcal{L} is defined by

$$\mathcal{L} = \exp\left(-\sum_{i=1}^7 n_i\right) \prod_{j=1}^N \left[\sum_{i=1}^7 n_i \mathcal{P}_i \right], \quad (1)$$

where N is the number of observed events and n_i are the yields of the signal, continuum background, and five $B\bar{B}$ background categories from Sec. III B. Correlations between the three fitted observables are found to be small. Therefore, the functions \mathcal{P}_i are taken to be products of independent probability density functions (PDFs) for ΔE , m_{ES} , and $M_{K^+\pi^-}$. Effects related to residual correlations are incorporated through the bias correction and systematic uncertainties discussed below.

The signal PDFs are defined by a double Gaussian distribution for ΔE , a Crystal Ball function [16] for m_{ES} , and a Breit-Wigner function for $M_{K^+\pi^-}$. The parameters are fixed to values found from fitting signal MC events. We verify that the signal MC predictions for the ΔE and m_{ES} distributions agree with the measured results from $B^0 \rightarrow \phi K_S^0$ decays [17] to within the experimental statistical uncertainties. The ϕK_S^0 channel is chosen for this purpose because of its similarity to the $\bar{K}^{*0}K_S^0$ channel.

Separate PDFs are determined for the continuum background and all five categories of $B\bar{B}$ background. The background PDFs are defined by combinations of polynomial, Gaussian, ARGUS [18], and Breit-Wigner functions fitted to MC events, with the exception of the PDFs for the S -wave $K^\pm\pi^\mp$ component for which the ΔE and m_{ES} PDFs are set equal to those of the signal while the $M_{K^+\pi^-}$ PDF is based on the scalar $K\pi$ lineshape determined by the LASS Collaboration [19].

The event yields of the continuum and last two categories of $B\bar{B}$ background from Sec. III B are allowed to vary in the fits, while those of the first three categories of $B\bar{B}$ background are set equal to the expected numbers given in Sec. III B. The PDF shape parameters of the continuum events are allowed to vary in the fit, while those of the five $B\bar{B}$ background categories are fixed.

IV. RESULTS

We find 682 data events that satisfy the selection criteria. Application of the ML fit to this sample yields $1.0_{-3.9}^{+4.7}$ signal events and 660 ± 75 continuum events, where the uncertainties are statistical. These results and those for the $B\bar{B}$ background yields are given in Table II. Based on the SM branching fraction predictions of Ref. [2], 5 signal events (rounded to the nearest integer) are expected. The number of expected continuum events is 619. The statisti-

TABLE II. Results from the maximum likelihood fit. $B\bar{B}$ background categories 4 and 5 refer to the last two categories of background itemized in Sec. III B. The yields for the first three $B\bar{B}$ background categories in Sec. III B are fixed to the estimated values of 1.0 event each. The uncertainties on the yields, fit bias, and efficiencies are statistical.

Parameter	Value
Number of events	682
Signal yield	$1.0^{+4.7}_{-3.9}$
Continuum background yield	660 ± 75
$B\bar{B}$ background category 4 yield	17^{+74}_{-71}
$B\bar{B}$ background category 5 yield	$1.4^{+6.4}_{-5.3}$
ML fit bias (signal bias)	-0.2 ± 0.3
MC signal efficiency (including D^\mp and ϕ mass vetos)	$9.8 \pm 0.1\%$
Efficiency corrections	
K_S^0 tracking	97.8%
K^{*0} tracking	99.0%
Final-state branching fractions	23.0%
Overall detection efficiency	$2.2 \pm 0.1\%$
$\mathcal{B}(B^0 \rightarrow \bar{K}^{*0} K^0) + \mathcal{B}(B^0 \rightarrow K^{*0} \bar{K}^0)$	$(0.2^{+0.9+0.1}_{-0.8-0.3}) \times 10^{-6}$
Significance with systematics (σ)	0.26
90% CL upper limit on $\mathcal{B}(B^0 \rightarrow \bar{K}^{*0} K^0) + \mathcal{B}(B^0 \rightarrow K^{*0} \bar{K}^0)$	$< 1.9 \times 10^{-6}$

cal uncertainty of the signal yield is defined by the change in the number of events required to increase the quantity $-2 \ln \mathcal{L}$ by one unit from its minimum value, and similarly for the other yields. The statistical significance of the result, defined by the square root of the difference between the value of $-2 \ln \mathcal{L}$ for zero signal events and at its minimum, is 0.28σ .

Figure 2 shows distributions of the fitted variables. To enhance the visibility of a potential signal, events are required to satisfy $\mathcal{L}_i(S)/[\mathcal{L}_i(S) + \mathcal{L}_i(B)] > 0.6$, where $\mathcal{L}_i(S)$ is the likelihood function for signal events excluding the PDF of the plotted variable i , and $\mathcal{L}_i(B)$ is the corresponding term for all background components added together. The points with uncertainties show the data. The curves show projections of the ML fit with the likelihood ratio restriction imposed.

We evaluate potential bias by performing pseudoexperiments whereby Monte Carlo signal and $B\bar{B}$ background events are mixed with continuum background events generated directly from the PDFs according to the expected yields in the data. The resulting estimate for the bias is $N_{\text{bias}} = -0.2 \pm 0.3(\text{stat.})$ events, yielding a corrected signal yield of 1.2 events.

In our study, we can distinguish $\bar{K}^{*0} K^0$ from $K^{*0} \bar{K}^0$ events with the sign of the electric charge of the K^\pm . However, we do not know the flavor of the B meson (B^0 or \bar{B}^0) at decay. Therefore, the observed signal yield is related to the sum of the $B^0 \rightarrow \bar{K}^{*0} K^0$ and $B^0 \rightarrow K^{*0} \bar{K}^0$ branching fractions through

$$\mathcal{B}(B^0 \rightarrow \bar{K}^{*0} K^0) + \mathcal{B}(B^0 \rightarrow K^{*0} \bar{K}^0) = \frac{N_{\text{sig}} - N_{\text{bias}}}{\epsilon N_{B\bar{B}}}, \quad (2)$$

where ϵ is the overall detection efficiency and $N_{B\bar{B}}$ is the number of $B\bar{B}$ events in the initial data sample. We assume equal decay rates of the $Y(4S)$ to $B^0 \bar{B}^0$ and $B^+ B^-$. The efficiency is given by the product of the MC signal efficiency and three efficiency corrections (Table II). The K_S^0 and K^{*0} tracking corrections account for discrepancies between the data and MC simulation. The K_S^0 efficiency correction is determined using inclusive samples of continuum and $B\bar{B}$ events, from a comparison of the efficiency to reconstruct K_S^0 mesons as a function of the transverse momentum, polar angle, and transverse flight distance with respect to the beam axis. The tracking efficiency correction for all other tracks, and thus for the K^{*0} decay products, is determined by comparing the tracking efficiency in data and MC for samples of τ events. The correction for final-state branching fractions accounts for the $K_S^0 \rightarrow \pi^+ \pi^-$ and $K^{*0} \rightarrow K^+ \pi^-$ branching fractions and for the fact that only one half of the K^0 mesons decay as a K_S^0 (these effects are not incorporated into the simulated signal event sample). The overall efficiency is $\epsilon = 2.2\%$.

We find the sum of the branching fractions to be $\mathcal{B}(B^0 \rightarrow \bar{K}^{*0} K^0) + \mathcal{B}(B^0 \rightarrow K^{*0} \bar{K}^0) = (0.2^{+0.9+0.1}_{-0.8-0.3}) \times 10^{-6}$, where the first uncertainty is statistical and the second is systematic. The systematic uncertainty is discussed in Sec. V. We determine a Bayesian 90% confidence level (CL) upper limit assuming a uniform prior probability distribution. First, the likelihood function is modified to incorporate systematic uncertainties through convolution with a Gaussian distribution whose standard deviation is set equal to the total systematic uncertainty. The 90% CL upper limit is defined by the value of the branching fraction below which lies 90% of the integral of the modified likelihood function in the positive branching fraction region.

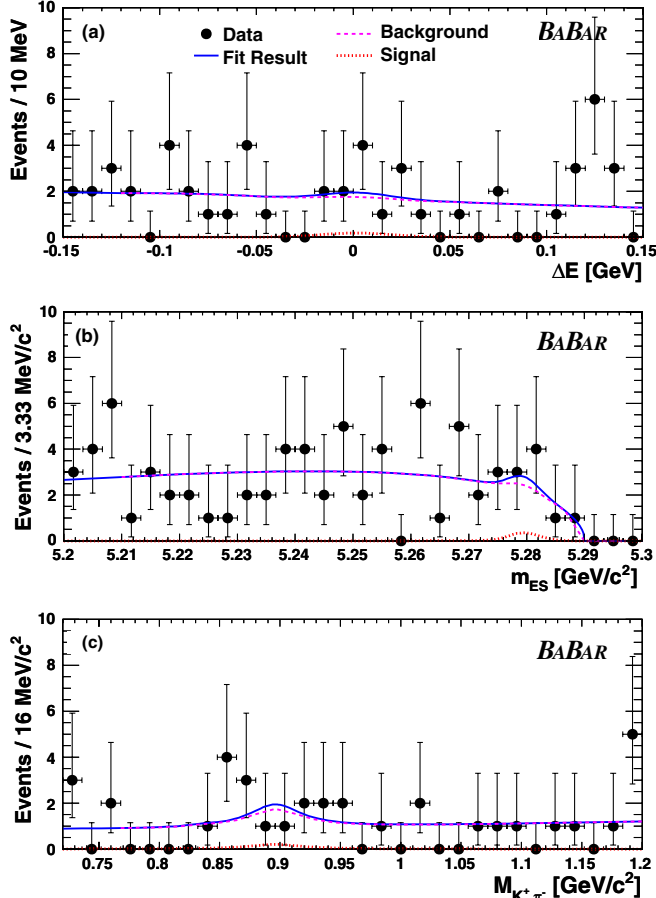


FIG. 2 (color online). Distributions of ΔE , m_{ES} , and $M_{K^+ \pi^-}$. The points with uncertainties show the data. The curves show projections of the ML fit. A selection requirement on the likelihood ratio has been applied as described in the text. The solid curve shows the sum of all fitted components, including the signal. The dashed curve shows the sum of all background components. The dotted curve (barely visible) shows the signal component.

We obtain $\mathcal{B}(B^0 \rightarrow \bar{K}^{*0} K^0) + \mathcal{B}(B^0 \rightarrow K^{*0} \bar{K}^0) < 1.9 \times 10^{-6}$. The modified likelihood function is used to determine the significance of the branching fraction result including systematics and is found to be 0.26σ .

V. SYSTEMATIC UNCERTAINTIES

Our evaluation of systematic uncertainties is summarized in Table III.

To estimate the systematic uncertainty related to the signal PDFs, we independently vary the corresponding parameters. The mean and standard deviation of the central ΔE Gaussian distribution, and the mean of the m_{ES} Crystal Ball function, are varied by the statistical uncertainties found by fitting the corresponding quantities to data in $B^0 \rightarrow \phi K^0$ decays [17]. We vary the standard deviation of the m_{ES} Crystal Ball function to account for observed variations between different run periods. The width of the

TABLE III. Summary of systematic uncertainties.

Systematic effect	Uncertainty
ML fit procedure (events)	
Signal PDF parameters	0.5
Fit bias	0.5
$B\bar{B}$ background yields	0.1
Total uncertainty from ML fit (events)	0.7
Scalar $K\pi$ lineshape (events)	+0.0 -1.4
Efficiency corrections (%)	
K_S^0 reconstruction	1.4%
K^{*0} tracking	2.8%
K^{*0} Particle identification	0.8%
$\cos\theta_T$ selection requirement	5.0%
Number of $B\bar{B}$ pairs	1.1%
$\mathcal{B}(K_S^0 \rightarrow \pi^+ \pi^-)$	0.1%
Total uncertainty from corrections	6.1%
Total systematic uncertainty for $\mathcal{B}(\times 10^6)$	+0.1 -0.3

$M_{K^+ \pi^-}$ Breit-Wigner function is varied by $\pm 0.01 \text{ GeV}/c^2$. The remaining signal PDF parameters are varied by the 1 standard deviation statistical uncertainties found in the fits to MC distributions (Sec. III C), taking into account correlations between parameters. The percentage change in the signal yield compared to the standard fit is taken as a parameter's contribution to the overall uncertainty. The contributions from all parameters are added in quadrature.

The systematic uncertainty of the fit bias is defined by adding two terms in quadrature. The first term is the statistical uncertainty of this bias (Table II). The second term is defined by evaluating the fit bias using the PDFs for the fourth $B\bar{B}$ background category (Sec. III B) rather than MC events. This category of events is chosen because it dominates the $B\bar{B}$ background. The difference between the corrected mean signal yield and the standard result defines the second term.

To estimate an uncertainty associated with the $B\bar{B}$ background, we vary the assumed numbers of events for the three $B\bar{B}$ background categories for which these numbers are fixed, i.e., the first three background categories of Sec. III B. Specifically, we independently vary these numbers by +2 and -1 events from their standard values of 1 event, and determine the quadrature sum of the resulting changes in the signal yield.

A systematic uncertainty associated with the presumed scalar $K\pi$ lineshape is defined by the difference between the signal yield found using the LASS lineshape and a uniform (i.e., flat) $K\pi$ mass distribution.

Systematic uncertainties for the K_S^0 and K^{*0} reconstruction efficiency corrections, and for the particle identification efficiency of the K^{*0} decay products, account for known discrepancies between the data and MC simulation. The systematic uncertainties for the particle identification efficiency are evaluated using data control samples such as

$D^{*+} \rightarrow D^0 \pi^+ \rightarrow K^- \pi^+ \pi^+$, in which the charge of the ‘‘slow’’ π^+ from the direct D^{*+} decay identifies the charged kaon and pion from the D^0 decay. The MC simulation is known to overestimate the number of events with $|\cos\theta_T| < 0.9$. We assign a 5% systematic uncertainty to account for this effect.

The systematic uncertainty associated with the number of $B\bar{B}$ pairs is 1.1%. The uncertainty of the $K_S^0 \rightarrow \pi^+ \pi^-$ branching fraction is taken from Ref. [6].

The total systematic uncertainty is defined by adding the above-described items in quadrature.

VI. SUMMARY AND DISCUSSION

In this paper, we present the first experimental results for the decay $B^0(\bar{B}^0) \rightarrow \bar{K}^{*0} K^0$. From a sample of about 232×10^6 $B\bar{B}$ events, we observe $1.2_{-3.9}^{+4.7}$ $B^0 \rightarrow \bar{K}^{*0} K^0$ event candidates. (This result includes the estimated signal bias of 0.2 events.) The corresponding measured sum of branching fractions is $\mathcal{B}(B^0 \rightarrow \bar{K}^{*0} K^0) + \mathcal{B}(B^0 \rightarrow K^{*0} \bar{K}^0) = (0.2_{-0.8-0.3}^{+0.9+0.1}) \times 10^{-6}$. We obtain a 90% confidence level upper limit of $\mathcal{B}(B^0 \rightarrow \bar{K}^{*0} K^0) + \mathcal{B}(B^0 \rightarrow K^{*0} \bar{K}^0) < 1.9 \times 10^{-6}$.

Our result can be used to determine an upper bound on $\Delta S_{\phi K^0}$, as mentioned in the introduction. As described in Ref. [7], $\Delta S_{\phi K^0}$ is given by

$$\Delta S_{\phi K^0} = 2 \cos 2\beta \sin \gamma \cos \delta |\xi_{\phi K^0}|, \quad (3)$$

with

$$\xi_{\phi K^0} \equiv \frac{V_{ub}^* V_{us} a^u}{V_{cb}^* V_{cs} a^c}, \quad (4)$$

with $a^c = p^c - p^t$ and $a^u = p^u - p^t$, where p^i is the hadronic amplitude of the penguin diagram with intermediate quark $i = u, c$ or t in $B^0 \rightarrow \phi K^0$ decays, and where δ and γ are the strong and weak phase differences, respectively, between a^u and a^c .

In the method of Grossman *et al.* [7], a bound on $\xi_{\phi K^0}$ is derived using the branching fractions of 11 strangeness-conserving charmless B^0 decays:

$$|\hat{\xi}_{\phi K^0}| \leq \left| \frac{V_{us}}{V_{ud}} \right| \left\{ 0.5 \sqrt{\frac{2[\mathcal{B}(\bar{K}^{*0} K^0) + \mathcal{B}(K^{*0} \bar{K}^0)]}{\mathcal{B}(\phi K^0)}} + \sum_{i=1}^9 C_i \sqrt{\frac{\mathcal{B}(f_i)}{\mathcal{B}(\phi K^0)}} \right\}, \quad (5)$$

where $\hat{\xi}_{\phi K^0}$ is related to $\xi_{\phi K^0}$ through [7,20]

$$|\hat{\xi}_{\phi K^0}|^2 = \frac{|V_{us} V_{cd} / V_{cs} V_{ud}|^2 + |\xi_{\phi K^0}|^2 + 2 \cos \gamma \operatorname{Re} \left(\frac{V_{us} V_{cd}}{V_{cs} V_{ud}} \xi_{\phi K^0} \right)}{1 + |\xi_{\phi K^0}|^2 + 2 \cos \gamma \operatorname{Re}(\xi_{\phi K^0})}. \quad (6)$$

The C_i are $SU(3)$ coefficients while the nine final states

$f_i = hh'$ are specified by $h = \phi, \omega$ or ρ^0 and $h' = \eta, \eta'$ or π^0 .

We evaluate a 90% CL upper limit on $|\Delta S_{\phi K^0}|$ by generating hypothetical sets of branching fractions for the 11 required $SU(3)$ -related decays. Branching fraction values are chosen using bifurcated Gaussian probability distribution functions with means and bifurcated widths set equal to the measured branching fractions and asymmetric uncertainties. For the measurements of the branching fractions of the nine channels not included in the present study, see Refs. [21,22]. Note that there are not statistically significant signals for any of these channels. Negative generated branching fractions are discarded. For each set of hypothetical branching fractions, we compute a bound on $|\Delta S_{\phi K^0}|$ using Eqs. (3) and (5). For the unknown phase term $\cos \delta$ in Eq. (3), we sample a uniform distribution between -1 and 1 . Similarly, the weak phase angle γ is chosen by selecting values from a uniform distribution between 38 and 79 degrees, corresponding to the 95% confidence level interval for γ given in Ref. [23]. (A flat distribution is chosen for γ because the likelihood curve in Ref. [23] is non-Gaussian.) We use $\sin 2\beta = 0.687$ [22]. For each iteration of variables, Eq. (6) is solved numerically for $|\xi_{\phi K^0}|$.

We find that 90% of the hypothetical $|\Delta S_{\phi K^0}|$ bounds lie below 0.42 and thereby determine $|\Delta S_{\phi K^0}| < 0.42$ at 90% CL. This is the first determination of this bound based on the method of Ref. [7]. As a cross check, we also determine the $SU(3)$ bound assuming the weak phase angle γ to be distributed according to a Gaussian distribution with a mean of 58.5° and a standard deviation of 5.8° [24]: this yields $|\Delta S_{\phi K^0}| < 0.43$ at 90% CL. The method of Ref. [7] does not account for $SU(3)$ flavor breaking effects, generally expected to be on the order of 30%. However, the method is conservative in that it assumes all hadronic amplitudes interfere constructively.

ACKNOWLEDGMENTS

We are grateful for the extraordinary contributions of our PEP-II colleagues in achieving the excellent luminosity and machine conditions that have made this work possible. The success of this project also relies critically on the expertise and dedication of the computing organizations that support *BABAR*. The collaborating institutions wish to thank SLAC for its support and the kind hospitality extended to them. This work is supported by the US Department of Energy and National Science Foundation (Canada), Institute of High Energy Physics (China), the Commissariat à l’Energie Atomique and Institut National de Physique Nucléaire et de Physique des Particules (France), the Bundesministerium für Bildung und Forschung and Deutsche Forschungsgemeinschaft (Germany), the Istituto Nazionale di Fisica Nucleare

(Italy), the Foundation for Fundamental Research on Matter (The Netherlands), the Research Council of Norway, the Ministry of Science and Technology of the Russian Federation, and the Particle Physics and Astronomy Research Council (United Kingdom).

Individuals have received support from CONACyT (Mexico), the Marie-Curie IEF (European Union), the A. P. Sloan Foundation, the Research Corporation, and the Alexander von Humboldt Foundation.

-
- [1] A. Ali, G. Kramer, and C.-D. Lü, *Phys. Rev. D* **58**, 094009 (1998); Y.-H. Chen, H.-Y. Cheng, B. Tseng, and K.-C. Yang, *Phys. Rev. D* **60**, 094014 (1999); N. G. Deshpande, B. Dutta, and S. Oh, *Phys. Lett. B* **473**, 141 (2000); M. Beneke and M. Neubert, *Nucl. Phys.* **B675**, 333 (2003).
 - [2] C.-W. Chiang, M. Gronau, Z. Luo, J. L. Rosner, and D. A. Suprun, *Phys. Rev. D* **69**, 034001 (2004).
 - [3] R. Wang, G. R. Lu, E.-K. Wang, and Y.-D. Yang, *Eur. Phys. J. C* **47**, 815 (2006).
 - [4] E. Eckhart *et al.* (CLEO Collaboration), *Phys. Rev. Lett.* **89**, 251801 (2002); A. Garmash *et al.* (BELLE Collaboration), *Phys. Rev. D* **69**, 012001 (2004).
 - [5] R. Fleischer and S. Recksiegel, *Phys. Rev. D* **71**, 051501(R) (2005).
 - [6] S. Eidelman *et al.* (Particle Data Group), *Phys. Lett. B* **592**, 1 (2004).
 - [7] Y. Grossman, Z. Ligeti, Y. Nir, and H. Quinn, *Phys. Rev. D* **68**, 015004 (2003).
 - [8] B. Aubert *et al.* (BABAR Collaboration), *Nucl. Instrum. Methods Phys. Res., Sect. A* **479**, 1 (2002).
 - [9] D. Lange, *Nucl. Instrum. Methods Phys. Res., Sect. A* **462**, 152 (2001).
 - [10] T. Sjöstrand, *Comput. Phys. Commun.* **82**, 74 (1994).
 - [11] The BABAR detector simulation is based on GEANT4; see *Nucl. Instrum. Methods Phys. Res., Sect. A* **506**, 250 (2003).
 - [12] For more detail, see, e.g., B. Aubert *et al.* (BABAR Collaboration), *Phys. Rev. D* **70**, 032006 (2004).
 - [13] S. Brandt *et al.*, *Phys. Lett.* **12**, 57 (1964); E. Farhi, *Phys. Rev. Lett.* **39**, 1587 (1977).
 - [14] R. A. Fisher, *Annals of Eugenics* **7**, 179 (1936); see also G. Cowan, *Statistical Data Analysis* (Oxford University Press, New York, 1998).
 - [15] A. Garmash *et al.* (BELLE Collaboration), *Phys. Rev. D* **71**, 092003 (2005); B. Aubert *et al.* (BABAR Collaboration), *Phys. Rev. D* **72**, 072003 (2005).
 - [16] T. Skwarnicki *et al.* (Crystal Ball Collaboration), DESY Report No. DESY-F31-86-02, 1986 (unpublished).
 - [17] B. Aubert *et al.* (BABAR Collaboration), *Phys. Rev. D* **71**, 091102 (2005).
 - [18] H. Albrecht *et al.* (ARGUS Collaboration), *Z. Phys. C* **48**, 543 (1990).
 - [19] D. Aston *et al.* (LASS Collaboration), *Nucl. Phys.* **B296**, 493 (1988).
 - [20] G. Engelhard, Y. Nir, and G. Raz, *Phys. Rev. D* **72**, 075013 (2005).
 - [21] B. Aubert *et al.* (BABAR Collaboration), *Phys. Rev. Lett.* **93**, 181806 (2004); **95**, 131803 (2005); *Phys. Rev. D* **70**, 032006 (2004).
 - [22] E. Barberio *et al.* (Heavy Flavor Averaging Group), hep-ex/0603003; The results for the $B^0 \rightarrow \rho^0 \pi^0$ branching fraction are taken from Table 36.
 - [23] J. Charles *et al.* (CKMfitter Group), *Eur. Phys. J. C* **41**, 1 (2005).
 - [24] M. Bona *et al.* (UTfit Collaboration), *J. High Energy Phys.* **07** (2005) 028.